ELSEVIER

Physica B 283 (2000) 157–161

PHYSICA B

www.elsevier.com/locate/physb

Roughness in sputtered multilayers analyzed by transmission electron microscopy and X-ray diffuse scattering

A.T. Macrander[a,*], C. Liu[a], R. Csencsits[b], R. Cook[b], M. Kirk[b], R. Headrick[c]

[a]*Advanced Photon Source, Argonne National Laboratory, Building 401, room B3164, Argonne, IL 60439, USA*
[b]*Materials Science Division, Argonne National Laboratory, Argonne, IL, USA*
[c]*Cornell High Energy Synchrotron Source, Cornell University, Ithaca, NY, USA*

Abstract

Sputtered W/C multilayers with a period of 25 Å have been studied both by cross-section TEM and by X-ray diffuse scattering using 10 keV synchrotron radiation. Fitting to the X-ray data is aided by the TEM images in modeling the roughness and roughness propagation within the Born approximation. We report on a study of the correctness of the often applied small roughness approximation, and we find that is not well justified in the present case. In order to probe short lateral length scales at $q_y = 0.1$ Å^{-1}, diffuse scattering data were obtained in an unconventional scattering geometry.

PACS: 41.50. + h; 61.10. − i; 61.10.Kw; 81.15.Aa

Keywords: X-ray; Diffuse scattering; Roughness; Correlation

1. Introduction

Multilayer optics are useful as monochromators and analyzers for synchrotron radiation beamlines. The angular acceptance and energy bandpass fall into an entirely different class when compared to those available with crystal optics. Typical values for multilayers are 1000 times larger compared to crystals [1]. Largely because of their roughness continuous sputtered films are limited to a smallest thickness slightly less than 10 Å and for this reason, Bragg angles of the first-order reflection for hard X-rays are 1.8° at most. To make multilayer optics more useful for hard X-rays one must drive the deposition technology towards achieving high reflectivity with the thinnest possible layers so that the first order reflectivity occurs at a q_z, the momentum transfer normal to the surface, that is as high as possible. For this reason the conventional "small roughness" approximation $[\exp(q_z^2 C) \cong 1 + q_z^2 C]$, where C is the interface height–height correlation function is naturally called into question. As part of a project to produce a cooled monochromator optic for the Cornell high-energy synchrotron source (CHESS), a detailed study of the scattering properties of a set of W/C multilayers was made at the CHESS F3 beamline. Multilayer coatings were DC magnetron sputtered in the deposition facility of the advanced photon source (APS) [2,3].

2. Sample details

Specular X-ray performance is detailed in Table 1 and has been reported elsewhere [4].

A cross section transmission electron micrograph is shown in Fig. 1. The electron microscopy was done at Argonne [5]. The TEM data reveal a quite regular interface progression for the whole 100 bilayer stack, and the interface conformality appears by eye to die out after ~ 2–3 bilayers.

Specimens for TEM analysis were prepared by glueing two pieces face-to-face using M-bond 610 adhesive.

*Corresponding author. Tel.: 630-252-5672; fax: 630-252-9303.

E-mail address: macrander@aps.anl.gov (A.T. Macrander)

0921-4526/00/$ - see front matter
PII: S0921-4526(99)01918-3

Table 1
Performance of W/C multilayer (10 keV)

Substrate	First-order reflectivity	Bandpass
0.5 mm thick Si	78%	1.5%

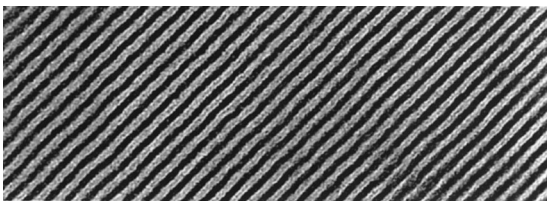

Fig. 1. Transmission electron micrograph of W/C multilayer. The W layers show as black bands. The bilayer spacing as determined from X-ray diffraction data is 25.3 Å.

A wire saw was used to cut thin slices which were subsequently ground and polished to 80 μm thickness using 3M diamond lapping films. The specimen was then dimpled and polished until the center of the specimen was less than 10 μm thick using a VCR dimpler. Final thinning to perforation was achieved using a Gatan PIPS low-angle ion mill.

TEM imaging was performed in the JEOL JEM 4000EXII high resolution transmission electron microscope operating at 400 kV. Images were taken with the silicon substrate in a $\langle 1\,1\,2\rangle$ orientation so that the W/C multilayer was viewed edge-on. Micrographs were recorded at 600 k× magnification on photographic film and subsequently digitized with a Leafscan 45 high-resolution negative scanner.

The layers are observed to be uniform in thickness throughout the thickness of the film and electron diffraction patterns indicate that both the carbon and tungsten are amorphous. Both the C/W and W/C interfaces appear abrupt.

3. Diffuse X-ray scattering

Conventionally, diffuse scattering experiments are performed by rocking the sample in the diffraction plane [6,7] (i.e., about an axis that is normal to the diffraction plane, as shown in Fig. 2) and this method has been applied to the study of W/C multilayers [8,9]. However, because either the incident beam or the scattered beam becomes grazing, this method is limited to lateral momentum transfers of $q_y \cong 0.02$ Å^{-1} (a value that applies to our samples for the second order). Momentum transfers roughly an order of magnitude larger can be investigated if one uses a scattering geometry whereby the sample normal is rotated out of the diffraction plane by an angle

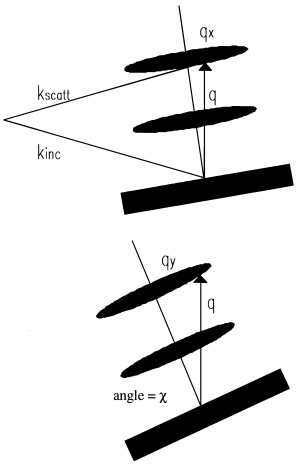

Fig. 2. The top panel (diffraction plane is in the plane of the paper) shows the more conventional procedure whereby the sample is rocked to probe a reciprocal lattice direction off of the specular condition. The bottom panel (diffraction plane is perpendicular to the plane of the paper) depicts the procedure used presently whereby a rotation by χ is made to rotate the sample normal out of the diffraction plane.

χ as also shown in Fig. 2. We used a goniometer with a conventional Eulerian cradle. We note that our procedure differs from that used by Salditt et al. [10] to access large in-plane momentum transfers. In their case only the detector arm is rotated during a scan.

Scanning along q_z was accomplished by a conventional θ–2θ scanning procedure where θ and 2θ are defined within the diffraction plane. These scans were always done for a symmetrical arrangement, i.e., the scattering angle, (2θ) was always equal to twice the θ angle. The resolution volume was calculated and also measured as detailed in Ref. [4].

The fundamental expression for the total scattering in the Born approximation is given by (see Ref. [7])

$$S(\boldsymbol{q}) = \frac{A}{q_z^2}\sum_{j,k}^{N} \mathrm{e}^{-q_z^2(\sigma_j^2+\sigma_k^2)/2}\Delta\rho_j\Delta\rho_k^*\mathrm{e}^{\mathrm{i}q_z(z_j-z_k)}\psi_{j,k}(\boldsymbol{q}), \tag{1}$$

where

$$\psi_{j,k}(\boldsymbol{q}) = 2\pi\iint \mathrm{d}X\,\mathrm{d}Y\,\mathrm{e}^{q_z^2C_{j,k}(X,Y)}\mathrm{e}^{-\mathrm{i}(q_xX+q_yY)}. \tag{2}$$

Here $C_{j,k}(X,Y) \equiv \langle u_j(X,Y)u_k(0,0)\rangle$ is the height–height correlation function between points on the jth and kth interface separated by the Cartesian distances X and Y, A is the illuminated area, $\Delta\rho$'s are the scattering length density contrast at an interface, z's are the average interface distance from the surface, and σ's are the interface roughnesses ($\sigma^2 = \langle u^2\rangle$). The sum in Eq. (1) must be performed over N interfaces. Eq. (2) is rigorously equal to the total (diffuse plus specular) scattering. To obtain the

diffuse part a unity term inside the integral in Eq. (2) must be subtracted. We prefer to treat the total scattering without having to correct it by subtracting the specular contribution. (We note that this unity subtraction is conventionally done whereby in conjunction with the small roughness approximation one obtains the result that $\psi_{j,k}$ becomes the Fourier Transform of the correlation function.) However, the specular contribution is very small at the large in-plane momentum transfers investigated presently so that we may still call the present work a study of diffuse scattering. $\psi_{j,k}$ can also be written as (see Ref. [6])

$$\psi_{j,k}(\boldsymbol{q}) = \int \mathrm{d}R\, R \mathrm{e}^{q_z^2 C_{j,k}}(R) J_0(q_r R). \tag{3}$$

Here $R \equiv (X^2 + Y^2)^{1/2}$, and $q_r \equiv (q_x^2 + q_y^2)^{1/2}$. The so-called "small roughness" approximation is often made which expands the exponential in Eq. (3) and keeps only the first two terms: $\exp(q_z^2 C_{j,k}) \cong 1 + q_z^2 C_{j,k}$. We have tested this approximation by performing the integral numerically both with and without this approximation. The oscillatory Bessel function in Eq. (3) complicates numerical integration. The method used to numerically carry out the integral in Eq. (3) was to first perform a Euler transformation involving terms integrating out to the 16th zero of J_0 [11]. This yielded good convergence as checked by comparing to results out to only the 15th zero of J_0.

To calculate $C_{j,k}$ we applied the accumulated roughness approach of Kaganer et al. [12] which relies on the following relationship for the roughness profile of the jth layer:

$$u_j(\boldsymbol{f}) = h_j(\boldsymbol{f}) + a_j(\boldsymbol{f}) u_{j+1}(\boldsymbol{f}). \tag{4}$$

This model of the roughness propagation is due to Stearns [13]. The second term in Eq. (4) represents the conformality of the jth interface with the interface below it multiplied by a damping factor. The first term in Eq. (4) represents the noise introduced by the sputtering of the jth layer. A spatial frequency (f) dependence for the lateral interface dimension is explicitly indicated.

As given by Kaganer et al. [12], the net result for $C_{j,k}$ is given by

$$C_{j,k}(\boldsymbol{\rho}) = \sum_{n \geq \max(j,k)} \frac{1}{\pi p_n^2} \int \mathrm{d}^2\rho' C_n(\rho')\, \mathrm{e}^{-(\rho' - \rho)^2/p_n^2}. \tag{5}$$

Here $p_n^2 = 4\nu(2z_n - z_j - z_k)$ and ρ represents a lateral Cartesion distance. The sum in Eq. (5) must be taken from the maximum of j,k down to the first-to-grow interface. (Indices increase from the surface down to the substrate.)

To obtain Eq. (5) a model for the damping factor has been applied given by

$$a_j(f) = \mathrm{e}^{-\nu(z_{j+1} - z_j) f^2}. \tag{6}$$

Eq. (5) can also be written as

$$C_{j,k}(\rho) = \sum_{n \geq \max(j,k)}^{N} \frac{2}{p_n^2} \int \mathrm{d}\rho'\, \rho' C_n(\rho') \mathrm{e}^{-((\rho')^2 + \rho^2)/p_n^2} I_0(2\rho\rho'/p_n^2). \tag{7}$$

Here I_0 is the zeroth-order modified Bessel function.

The development of Kaganer et al. [12] contains only a single type of interface, i.e., a single value of ν. The value of ν can be used to obtain a frequency dependent vertical correlation length over which interface conformality is damped out. Any real multilayer contains two types of interfaces and these are not necessarily the same. In general, the two types of interfaces will propagate roughness differently. Accordingly we introduce ν_o and ν_e for interfaces having either odd (C on W) or even numbered (W on C) indices. Our result is that Eq. (5) again applies but with a different expression for p_n^2. The new expression contains the individual layer thicknesses, a (W, 10.0 Å) and b (C, 15.3 Å), that make up a bilayer. It is

$$p_n^2 = 4(\tfrac{1}{2}[\nu_0 a + \nu_e b](2n - j - k) - \tfrac{1}{2}[\nu_0 a - \nu_e b]((-1)^k + (-1)^{n-1})). \tag{8}$$

The integral in Eq. (7) can be performed in closed form if the correlation function for the noise contribution arising from sputtering has a self-affine form with a roughness exponent (see Ref. [6]) equal to unity and contains a lateral correlation length, ξ. This correlation function is given by

$$C_n(\rho) = \sigma_n^2 \mathrm{e}^{-(\rho/\xi_n)^2} \tag{9}$$

By applying Eq. (9) into Eq. (7) one obtains (see Ref. [12])

$$C_{j,k}(\rho) = \sum_{n \geq \max(j,k)}^{N} \frac{\sigma_n^2}{(1 + p_n^2/\xi_n^2)} \mathrm{e}^{-\rho^2/(\xi_n^2 + p_n^2)} \tag{10}$$

The above equations were applied to achieve the results shown in Figs. 3 and 4. Results for each calculated scan took 18 h on a Sun Ultra workstation. (We note that this time is reduced very significantly for multilayers having fewer than the 200 layers that applies to the present case.) Although inconsequential, absorption and refraction were included. Also incorporated is a q_z^{-1} dependence of the total cross section due to the changing size of the illuminated area during a scan.

The difference between the best fit, case A, without (shown in Fig. 3) and with the small roughness approximation (shown in Fig. 4) is dramatic. We conclude that the small roughness approximation is not well justified presently.

For case B the only change from case A is that the in-plane correlation lengths, ξ_o and ξ_e, are only 2 Å larger, yet there is a remarkably large change in the calculated $S(q)$ evident in Fig. 4. We conclude that the fitting is very sensitive to the in-plane correlation lengths.

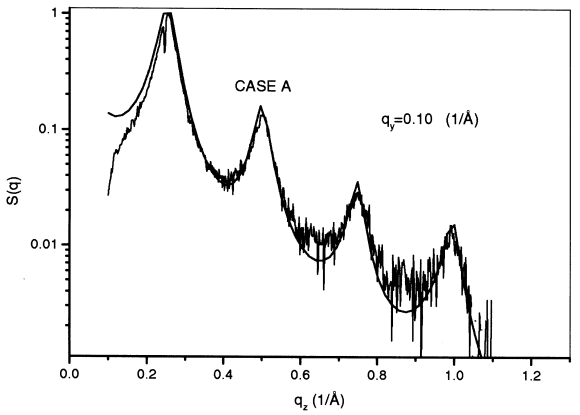

Fig. 3. Diffuse scattering data for $q_y = 0.10$ Å^{-1} and fit using Eqs. (1), (3)–(6), (8), (10). The fitting parameters are shown in Table 2 as case A.

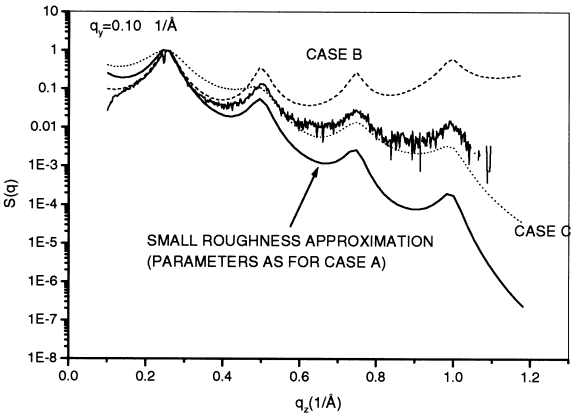

Fig. 4. Results obtained for deviations from best fit conditions (cases B and C) and for the "small roughness" approximation with parameters as for case A. The cases were individually normalized.

Table 2
Parameters for cases shown in Figs. 3 and 4. All quantities are in units of Å. Values subscripted as "s" refer to the substrate

Cases	A	B	C
σ_o	2.8	2.8	2.8
σ_e	2.8	2.8	2.8
σ_s	1.5	1.5	1.5
ξ_o	4.0	6.0	4.0
ξ_e	4.0	6.0	4.0
ξ_s	120.0	120.0	120.0
v_o	2.5	2.5	2.5
v_e	0.5	0.5	2.5

By having different values of the vertical roughness damping factors for each interface, we were able to obtain better fits than we could if we were constrained to have the same value for both types interfaces. Case C was chosen to demonstrate this finding. For case C the only change from case A is that the two vertical roughness damping factors, v_o and v_e, are set equal, and we find quite a significant deviation of $S(q)$ from the best fit result as is demonstrated in Fig. 4.

4. Conclusions

We conclude that the small roughness approximation is not well justified in the present case of very thin bilayer spacings.

Furthermore, the in-plane correlation lengths of the correlation functions for the roughness introduced by the sputtering process itself is rather short. We find a value of 4.0 Å for both kinds of interfaces, and we find that the fits are very sensitive to these correlation lengths. Although such a small value may appear unphysical at first sight, we note that it applies to the additional roughness introduced by the sputtering of each layer and is not indicative of the total accumulated roughness physically present at an interface. In a primitive model of crystal growth, the random deposition model [14], the interface is uncorrelated laterally, i.e., with a null correlation length. More sophisticated models such as ballistic deposition, random deposition with relaxation, or models leading to the Edwards–Wilkinson equation include lateral correlation [14]. We are led to infer that the range of this correlation is comparable to the rms roughness amplitude introduced by the sputtering of each layer.

Finally, we find an asymmetry between the damping of roughness propagation for the two types of interfaces. This damping acts in a spatial frequency-dependent way. For the C on W interface it is $v_o = 2.5$ Å which corresponds to a vertical correlation length of a single bilayer spacing at 8 Å spatial wavelength. For the W on C interface it is $v_e = 0.5$ Å which corresponds to a vertical correlation length of 5 bilayer spacings at 8 Å spatial wavelength, a 5 times larger value. For a TEM study of a W/C multilayer having a 60 Å bilayer spacing, Petford-Long et al. [15] report that W on C interfaces are considerably rougher than C on W. Although such an asymmetry in the roughness of the two types of interfaces is not evident in our TEM data (25 Å bilayer spacing), our X-ray diffuse scattering results do support an inherent asymmetry in the degree to which roughness can be propagated across the two types of interfaces.

Acknowledgements

One of us (A.T.M.) acknowledges several illuminating discussions with S.K. Sinha. This work was supported by

the US Dept. of Energy, Basic Energy Sciences, Office of Science, under contract No. W-31-109-ENG-38 and by the US National Science Foundation which supports CHESS under award number DMR-9713424.

References

[1] E. Spiller, Soft X-ray Optics, SPIE Engineering Press, Bellingham, WA, 1994.
[2] C. Liu, J. Erdmann, A. Macrander, The APS Coating Facilities, SRI-CAT Newsletter, April 1997, Vol. 3, pp. 2–4, http://www.aps.anl.gov/sricat/news.html.
[3] A.T. Macrander, L. Assoufid, C. Liu, C. Krasnicki, A. Khounsary, Optics fabrication and metrology group: status and capabilities, Advanced Photon Source CAT Communicator, Vol. 7, September 1997, pp. 11–15.
[4] A.T. Macrander, R.L. Headrick, C. Liu, J. Erdmann, A. Khounsary, K. Smolenski, S. Krasnicki, J. Maj, SPIE Proc. 3448 (1998) 291.
[5] M. Kirk, R. Csencsits, R. Cook, private communication.
[6] S.K. Sinha, E.B. Sirota, S. Garoff, H.B. Stanley, Phys. Rev. B 38 (1988) 2297.
[7] S.K. Sinha, J. Phys. (France) III 4 (1994) 1543.
[8] D.E. Savage, N. Schimke, Y.-H. Phang, M.G. Lagally, J. Appl. Phys. 71 (1992) 3283.
[9] D.E. Savage, J. Kleiner, N. Schimke, Y.-H. Phang, T. Jankowski, J. Jacobs, R. Kariotis, M.G. Lagally, J. Appl. Phys. 69 (1991) 1412.
[10] T. Salditt, T.H. Metzger, Ch. Brandt, U. Klemradt, J. Peisl, Phys. Rev. B 51 (1995) 5617.
[11] P.J. Davis, P. Rabinowitz, Methods of Numerical Integration, Academic Press, New York, 1984, p. 230.
[12] V.M. Kaganer, S.A. Stepanov, R. Kohler, Physica B 221 (1996) 34.
[13] D.G. Stearns, J. Appl. Phys. 71 (1992) 4286.
[14] A.-L. Barabasi, H.E. Stanley, Fractal Concepts in Surface Growth, Cambridge University Press, Cambridge, 1995 (Chapters 4 and 5).
[15] A.K. Petford-Long, MB. Stearns, C.-H. Chang, S.R. Nutt, D.G. Stearns, N.M. Ceglio, A.M. Hawryluk, J. Appl. Phys. 61 (1987) 1422.